JOURNAL OF MAGNETIC RESONANCE **128,** 12–20 (1997)
ARTICLE NO. MN971204

Detection of Double and Four Quantum Coherences for Spin $\frac{7}{2}$ Excited by Spin Lock Pulse Sequences

S. Z. Ageev,* P. P. Man,† and B. C. Sanctuary*

*Department of Chemistry, McGill University, Montreal, Quebec, H3A 2K6, Canada; and †Laboratorie de Chimie des Surfaces, CNRS URA 1428, Universite Pierre et Marie Curie, 4 Place Jussieu Tour 55, 75252 Paris Cedex 05, France

Received January 15, 1997; revised May 2, 1997

The response of a spin $\frac{7}{2}$ in solids, subject to a first-order quadrupolar interaction, to a spin lock pulse sequence is calculated. The results are valid for any ratio of quadrupolar coupling, ω_Q, to the amplitude, ω_1, of the RF pulse. It is shown here that the measurements of the central line intensity as a function of the second pulse length can be used for the determination of quadrupolar parameters using various phase cycling techniques. It is proven that the DQ coherences developed during the first pulse can be selectively detected.

INTRODUCTION

Investigation of multiquantum (MQ) coherences has received a great deal of interest in NMR (*1–7*). Spins of value higher than $\frac{1}{2}$ with quadrupolar splitting are multilevel systems with unequal spacing between the energy levels. As a result, a single RF pulse acts selectively, being resonant to a certain transition. A pulse which is applied to a single quantum (SQ) transition may excite other off-resonance SQ transitions as well as the MQ coherences. However, MQ transitions are not detected in this type of experiment, but these can be studied by using various pulse techniques. Particularly, double quantum (DQ) transitions in spin $\frac{3}{2}$ systems are well investigated by a combination of multipulse techniques with two-dimensional NMR (*8*); a combination of spin lock and rotary echo pulse sequences (*9*); and spin echo pulse sequences (*10*).

Application of computer algebra eases the calculations for spins higher than $\frac{3}{2}$ as it allows for efficient matrix manipulations. Recently, explicit analytical expressions were reported for spin $\frac{5}{2}$ (*11*) and spin $\frac{7}{2}$ (*12*) for two-pulse experiments with time delay between pulses. These solutions indicate that under soft pulse excitation conditions, which retain the first-order quadrupole, the MQ coherences, which are developed during the first pulse, are detected at the end of the second pulse as SQ coherences. Also Solomon echoes were calculated analytically for spin $\frac{5}{2}$ (*13*) and $\frac{7}{2}$ (*14*). Some of these echoes (''forbidden'' echoes) arise exclusively from the refocusing of MQ transitions.

In this paper we use the same pulse sequences employed for spins $\frac{3}{2}$ and $\frac{5}{2}$ in (*15*) to investigate MQ transitions for spin $\frac{7}{2}$. These two-pulse sequences include various phase cyclings as well as a combination of spin lock and spin echo pulse sequences. The first-order quadrupole is retained throughout and, in particular, in the calculations of pulses. Thus our results are applicable to symmetrical (i.e., featureless) lineshapes. However, the measurement of the integrated areas of the central line as a function of the second pulse length permits the determination of quadrupolar parameters and the true chemical shift of the line. The response of half-integer quadrupolar spins to two-pulse sequences as the function of the second pulse length has more extrema than that of one pulse. The shape of this curve is determined by the ratio of quadrupolar coupling, ω_Q, to the applied RF field in the case of a single crystal or by the ratio of quadrupolar coupling constant, $e^2qQ/\hbar$, to the applied RF field in the case of powders. Various two-pulse sequences produce different shapes of the response curve in question. This makes the fitting procedure more accurate as the results for quadrupolar parameters should be consistent for each experiment. The second-order effects are ignored in our treatment in contrast to (*16*) where second-order quadrupolar broadening is removed under MAS conditions by correlating multiple quantum and single quantum coherences. It should be noted that the central transition is broadened by second-order quadrupolar effects. In this paper we assume that the experiment would produce featureless spectra from which one can determine quadrupolar parameters.

THEORY

The Hamiltonian of the system excited by an RF pulse in the rotating frame associated with the central transition, and neglecting the offset and high frequency terms, is

$$H^{(\phi)} = H_Q^{(1)} + H_{\mathrm{RF}}^{(\phi)}, \qquad [1]$$

1090-7807/97 $25.00

where

$$H_Q^{(1)} = \frac{1}{3}\omega_Q[3I_z^2 - I(I+1)],$$

$$\omega_Q = \frac{3e^2qQ}{8I(2I-1)\hbar}(3\cos^2\beta - 1 + \eta\sin^2\beta\cos 2\alpha),$$

$$H_{\mathrm{RF}}^{(\phi)} = -\omega_1(I_x\cos\phi + I_y\sin\phi).$$

The Euler angles α and β describe the static magnetic field with respect to the quadrupolar principal axis system (QPAS); the RF amplitude ω_1 and phase ϕ describe the pulse. Here $H_Q^{(1)}$ is the first-order quadrupolar Hamiltonian, $e^2qQ/\hbar$ is the quadrupolar coupling constant, and η is the asymmetry parameter. The quadrupolar coupling ω_Q can be defined experimentally as one-half of the frequency difference which separates two consecutive lines in the spectrum of a single crystal. Angular frequency units are used, and the effects of relaxation and second-order quadrupole are ignored.

The dynamics of a spin $\frac{7}{2}$ excited by two RF pulses of arbitrary phases is given by the density matrix $\rho_{\phi_1,\phi_2}(t_1, t_2)$,

$$\rho_{\phi_1,\phi_2}(t_1, t_2) = \exp(-iH^{(\phi_2)}t_2)\exp(-iH^{(\phi_1)}t_1)\rho(0) \times \exp(iH^{(\phi_1)}t_1)\exp(iH^{(\phi_2)}t_2), \quad [2]$$

where

$$\rho(0) = I_z$$

and t_1, ϕ_1 and t_2, ϕ_2 are the durations and phases of the first and the second pulse, respectively.

DENSITY MATRIX AFTER ONE PULSE

Consider the dynamics of a spin $\frac{7}{2}$ excited by an RF pulse with an arbitrary phase ϕ. Note that

$$H_{RF}^{(\phi)} = \exp(-i\phi I_z)H_{\mathrm{RF}}^{(0)}\exp(i\phi I_z), \quad [3]$$

where $H_{\mathrm{RF}}^{(0)}$, $H_{\mathrm{RF}}^{(0)} = -\omega_1 I_x$, is the Hamiltonian of the RF pulse applied along the x axis. Thus using Eq. [1] one can write

$$H^{(\phi)} = \exp(-i\phi I_z)H^{(0)}\exp(i\phi I_z). \quad [4]$$

Then the density matrix for the system, $\rho_\phi(t_1)$, after an RF pulse of arbitrary phase ϕ is given by

$$\rho_\phi(t_1) = e^{-i\phi I_z}e^{-iH^{(0)}t_1}e^{i\phi I_z}I_z e^{-i\phi I_z}e^{iH^{(0)}t_1}e^{i\phi I_z} = e^{-i\phi I_z}\rho_0(t_1)e^{i\phi I_z}, \quad [5]$$

where $\rho_0(t_1)$ is the density matrix of the system excited by an $+x$ pulse. At this point it is easy to relate the density matrices after a pulse along the $+x$ axis, $\rho_0(t_1)$, and after a pulse along the $-x$ axis, $\rho_\pi(t_1)(\phi = \pi)$, viz.

$$\rho_\pi(t_1) = e^{-i\pi I_z}\rho_0(t_1)e^{i\pi I_z}. \quad [6]$$

Furthermore, the matrix I_z is diagonal in the $|I, M\rangle$ (M is the magnetic number) representation which simplifies the computation of Eqs. [5] and [6], giving

$$\langle k|\rho_\phi(t_1)|j\rangle = \langle k|\rho_0(t_1)|j\rangle\exp(i(k-j)\phi), \quad [7]$$

where $\langle k|\rho_\phi(t_1)|j\rangle$ and $\langle k|\rho_0(t_1)|j\rangle$ are matrix elements of matrices $\rho_\phi(t_1)$ and $\rho_0(t_1)$ located at the kth row and the jth column of their matrix representations. The immediate result which follows from Eqs. [6] and [7] is that only line intensities of odd quantum coherences change sign when the $-x$ pulse is changed to a $+x$ pulse and vice versa. Concurrently the polarizations and the even quantum coherences remain unchanged when the pulse phase is changed by 180°. In general, shifting the pulse phase by ϕ changes the phase of m-quantum coherences by $m\phi$ but the polarizations remain unchanged (see Eq. [7]). The matrix elements of $\rho_\pi(t_1)$ for spin $\frac{7}{2}$ have been calculated previously (*14, 16*). Making use of Eq. [7] allows the calculation of $\rho_{\pi/2}(t_1)$, the matrix form of which is given in Table 1, in notation described in (*16*). In the next section we use the results of Table 1 to calculate a response of the system in question to spin lock pulse sequences. However, it should be noted that the results represented by Eqs. [1]–[7] are valid for all half-integer spins.

DENSITY MATRIX FOR SPIN LOCKING SEQUENCES

The spin lock pulse sequence is composed of two RF pulses without time delays. The first pulse is applied along the y axis, whereas the second pulse is applied along the $-x$ axis. The density matrix after a spin lock pulse sequence is given by

$$\rho_{\pi/2,\pi}(t_1, t_2) = \exp(-iH^{(\pi)}t_2)\rho_{\pi/2}\exp(iH^{(\pi)}t_2). \quad [8]$$

The diagonalization procedure for $H^{(\pi)}$ has been discussed in detail in (*17*). Thus Eq. [8] can be developed using computer algebra ''Maple.'' However, in most cases only the central line is observed in experiments on powders. Thus below we focus on line intensity from this transition. The density matrix component

TABLE 1

The Density Matrix of Spin $\frac{7}{2}$ after the RF Pulse Applied along the y Axis

$$\begin{bmatrix}
\langle I_z^{1,8}\rangle & i\langle I_x^{1,2}\rangle + \langle I_y^{1,2}\rangle & -\langle I_x^{1,3}\rangle + i\langle I_y^{1,3}\rangle & -i\langle I_x^{1,4}\rangle - \langle I_y^{1,4}\rangle & \langle I_x^{1,5}\rangle - i\langle I_y^{1,5}\rangle & i\langle I_x^{1,6}\rangle + \langle I_y^{1,6}\rangle & -\langle I_x^{1,7}\rangle + i\langle I_y^{1,7}\rangle & -\langle I_y^{1,8}\rangle \\
-i\langle I_x^{1,2}\rangle + \langle I_y^{1,2}\rangle & \langle I_z^{2,7}\rangle & i\langle I_x^{2,3}\rangle + \langle I_y^{2,3}\rangle & -\langle I_x^{2,4}\rangle + i\langle I_y^{2,4}\rangle & -i\langle I_x^{2,5}\rangle - \langle I_y^{2,5}\rangle & \langle I_x^{2,6}\rangle - i\langle I_y^{2,6}\rangle & \langle I_y^{2,7}\rangle & \langle I_x^{1,7}\rangle + i\langle I_y^{1,7}\rangle \\
-\langle I_x^{1,3}\rangle - i\langle I_y^{1,3}\rangle & -i\langle I_x^{2,3}\rangle + \langle I_y^{2,3}\rangle & \langle I_z^{3,6}\rangle & i\langle I_x^{3,4}\rangle + \langle I_y^{3,4}\rangle & -\langle I_x^{3,5}\rangle + i\langle I_y^{3,5}\rangle & -\langle I_y^{3,6}\rangle & -\langle I_x^{2,6}\rangle - i\langle I_y^{2,6}\rangle & -i\langle I_x^{1,6}\rangle + \langle I_y^{1,6}\rangle \\
i\langle I_x^{1,4}\rangle - \langle I_y^{1,4}\rangle & -\langle I_x^{2,4}\rangle - i\langle I_y^{2,4}\rangle & -i\langle I_x^{3,4}\rangle + \langle I_y^{3,4}\rangle & \langle I_z^{4,5}\rangle & \langle I_y^{4,5}\rangle & \langle I_x^{3,5}\rangle + i\langle I_y^{3,5}\rangle & i\langle I_x^{2,5}\rangle - \langle I_y^{2,5}\rangle & -\langle I_x^{1,5}\rangle - i\langle I_y^{1,5}\rangle \\
\langle I_x^{1,5}\rangle + i\langle I_y^{1,5}\rangle & i\langle I_x^{2,5}\rangle - \langle I_y^{2,5}\rangle & -\langle I_x^{3,5}\rangle - i\langle I_y^{3,5}\rangle & \langle I_y^{4,5}\rangle & -\langle I_z^{4,5}\rangle & -i\langle I_x^{3,4}\rangle + \langle I_y^{3,4}\rangle & \langle I_x^{2,4}\rangle + i\langle I_y^{2,4}\rangle & i\langle I_x^{1,4}\rangle - \langle I_y^{1,4}\rangle \\
-i\langle I_x^{1,6}\rangle + \langle I_y^{1,6}\rangle & \langle I_x^{2,6}\rangle + i\langle I_y^{2,6}\rangle & -\langle I_y^{3,6}\rangle & \langle I_x^{3,5}\rangle - i\langle I_y^{3,5}\rangle & i\langle I_x^{3,4}\rangle + \langle I_y^{3,4}\rangle & -\langle I_z^{3,6}\rangle & -i\langle I_x^{2,3}\rangle + \langle I_y^{2,3}\rangle & \langle I_x^{1,3}\rangle + i\langle I_y^{1,3}\rangle \\
-\langle I_x^{1,7}\rangle - i\langle I_y^{1,7}\rangle & \langle I_y^{2,7}\rangle & -\langle I_x^{2,6}\rangle + i\langle I_y^{2,6}\rangle & -i\langle I_x^{2,5}\rangle - \langle I_y^{2,5}\rangle & \langle I_x^{2,4}\rangle - i\langle I_y^{2,4}\rangle & i\langle I_x^{2,3}\rangle + \langle I_y^{2,3}\rangle & -\langle I_z^{2,7}\rangle & -i\langle I_x^{1,2}\rangle + \langle I_y^{1,2}\rangle \\
-\langle I_y^{1,8}\rangle & \langle I_x^{1,7}\rangle - i\langle I_y^{1,7}\rangle & i\langle I_x^{1,6}\rangle + \langle I_y^{1,6}\rangle & -\langle I_x^{1,5}\rangle + i\langle I_y^{1,5}\rangle & -i\langle I_x^{1,4}\rangle - \langle I_y^{1,4}\rangle & \langle I_x^{1,3}\rangle - i\langle I_y^{1,3}\rangle & i\langle I_x^{1,2}\rangle + \langle I_y^{1,2}\rangle & -\langle I_z^{1,8}\rangle
\end{bmatrix}$$

$$\langle I_z^{1,8}\rangle = 2X_{1i}T_{2j}\cos\omega_{ij}t_1$$

$$\langle I_z^{2,7}\rangle = 2Y_{1i}Z_{2j}\cos\omega_{ij}t_1$$

$$\langle I_z^{3,6}\rangle = 2Z_{1i}Y_{2j}\cos\omega_{ij}t_1$$

$$\langle I_z^{4,5}\rangle = 2T_{1i}X_{2j}\cos\omega_{ij}t_1$$

$$\langle I_y^{1,8}\rangle = 2X_{1i}T_{2j}\sin\omega_{ij}t_1$$

$$\langle I_y^{2,7}\rangle = 2Y_{1i}Z_{2j}\sin\omega_{ij}t_1$$

$$\langle I_y^{3,6}\rangle = 2Z_{1i}Y_{2j}\sin\omega_{ij}t_1$$

$$\langle I_y^{4,5}\rangle = 2T_{1i}X_{2j}\sin\omega_{ij}t_1$$

$$\langle I_x^{1,2}\rangle + i\langle I_y^{1,2}\rangle = (X_{1i}Z_{2j} + Y_{1i}T_{2j})\cos\omega_{ij}t_1 + i(X_{1i}Z_{2j} - Y_{1i}T_{2j})\sin\omega_{ij}t_1$$

$$\langle I_x^{1,3}\rangle + i\langle I_y^{1,3}\rangle = (X_{1i}Y_{2j} + Z_{1i}T_{2j})\cos\omega_{ij}t_1 + i(X_{1i}Y_{2j} - Z_{1i}T_{2j})\sin\omega_{ij}t_1$$

$$\langle I_x^{1,4}\rangle + i\langle I_y^{1,4}\rangle = (X_{1i}X_{2j} + T_{1i}T_{2j})\cos\omega_{ij}t_1 + i(X_{1i}X_{2j} - T_{1i}T_{2j})\sin\omega_{ij}t_1$$

$$\langle I_x^{1,5}\rangle + i\langle I_y^{1,5}\rangle = (X_{1i}X_{2j} - T_{1i}T_{2j})\cos\omega_{ij}t_1 + i(X_{1i}X_{2j} + T_{1i}T_{2j})\sin\omega_{ij}t_1$$

$$\langle I_x^{1,6}\rangle + i\langle I_y^{1,5}\rangle = (X_{1i}Y_{2j} - Z_{1i}T_{2j})\cos\omega_{ij}t_1 + i(X_{1i}Y_{2j} + Z_{1i}T_{2j})\sin\omega_{ij}t_1$$

$$\langle I_x^{1,7}\rangle + i\langle I_y^{1,7}\rangle = (X_{1i}Z_{2j} - Y_{1i}T_{2j})\cos\omega_{ij}t_1 + i(X_{1i}Z_{2j} + Y_{1i}T_{2j})\sin\omega_{ij}t_1$$

$$\langle I_x^{2,3}\rangle + i\langle I_y^{2,3}\rangle = (Y_{1i}Y_{2j} + Z_{1i}Z_{2j})\cos\omega_{ij}t_1 - i(Y_{1i}Y_{2j} - Z_{1i}Z_{2j})\sin\omega_{ij}t_1$$

$$\langle I_x^{2,4}\rangle + i\langle I_y^{2,4}\rangle = (Y_{1i}X_{2j} + T_{1i}Z_{2j})\cos\omega_{ij}t_1 - i(Y_{1i}X_{2j} - T_{1i}Z_{2j})\sin\omega_{ij}t_1$$

$$\langle I_x^{2,5}\rangle + i\langle I_y^{2,5}\rangle = (Y_{1i}X_{2j} - T_{1i}Z_{2j})\cos\omega_{ij}t_1 + i(Y_{1i}X_{2j} + T_{1i}Z_{2j})\sin\omega_{ij}t_1$$

$$\langle I_x^{2,6}\rangle + i\langle I_y^{2,6}\rangle = (Y_{1i}Y_{2j} - Z_{1i}Z_{2j})\cos\omega_{ij}t_1 + i(Y_{1i}Y_{2j} + Z_{1i}Z_{2j})\sin\omega_{ij}t_1$$

$$\langle I_x^{3,4}\rangle + i\langle I_y^{3,4}\rangle = (Z_{1i}X_{2j} + T_{1i}Y_{2j})\cos\omega_{ij}t_1 + i(Z_{1i}X_{2j} - T_{1i}Y_{2j})\sin\omega_{ij}t_1$$

$$\langle I_x^{3,5}\rangle + i\langle I_y^{3,5}\rangle = (Z_{1i}X_{2j} - T_{1i}Y_{2j})\cos\omega_{ij}t_1 + i(Z_{1i}X_{2j} + T_{1i}Y_{2j})\sin\omega_{ij}t_1$$

Note. The functions $\langle I_k^{i,j}\rangle$ are reported in (*17*).

$\langle 5|\rho_{\pi/2,\pi}(t_1,t_2)|4\rangle$ which corresponds to the central transition is calculated to be

$$\begin{aligned}
\langle 5|\rho_{\pi/2,\pi}(t_1,t_2)|4\rangle = {} & -\langle I_y^{1,8}\rangle(D_1 + D_2) \\
& + \langle I_y^{2,7}\rangle(D_3 + D_4) - \langle I_y^{3,6}\rangle(D_5 + D_6) \\
& + \langle I_y^{4,5}\rangle(D_7 + D_8) - \langle I_y^{1,2}\rangle(V_1 - V_2) \\
& - \langle I_y^{1,4}\rangle(V_3 - V_4) + \langle I_y^{1,6}\rangle(V_5 + V_6) \\
& - \langle I_y^{2,3}\rangle(V_7 - V_8) - \langle I_y^{2,5}\rangle(V_9 + V_{10}) \\
& - \langle I_y^{3,4}\rangle(V_{11} - V_{12}) - \langle I_x^{1,2}\rangle(V_{13} + V_{14}) \\
& - \langle I_x^{1,4}\rangle(V_{15} + V_{16}) - \langle I_x^{1,6}\rangle(V_{17} + V_{18}) \\
& - \langle I_x^{2,3}\rangle(V_{19} + V_{20}) - \langle I_x^{2,5}\rangle(V_{21} + V_{22}) \\
& - \langle I_x^{3,4}\rangle(V_{23} + V_{24}) + i(\langle I_z^{3,6}\rangle C_5 + \langle I_z^{2,7}\rangle C_6 \\
& + \langle I_z^{1,8}\rangle C_7 + \langle I_z^{4,5}\rangle C_8 - \langle I_x^{3,5}\rangle(C_{10} - C_{12}) \\
& + \langle I_x^{2,6}\rangle(C_{14} - C_{16}) - \langle I_x^{2,4}\rangle(C_{18} + C_{20}) \\
& - \langle I_x^{1,7}\rangle(C_{22} - C_{24}) - \langle I_x^{1,3}\rangle(C_{26} + C_{28}) \\
& + \langle I_x^{1,5}\rangle(C_{30} - C_{32}) - \langle I_y^{3,5}\rangle(C_9 + C_{11}) \\
& + \langle I_y^{2,6}\rangle(C_{13} + C_{15}) - \langle I_y^{2,4}\rangle(C_{17} - C_{19}) \\
& - \langle I_y^{1,7}\rangle(C_{21} + C_{23}) - \langle I_y^{1,3}\rangle(C_{25} - C_{27}) \\
& + \langle I_y^{1,5}\rangle(C_{29} + C_{31})). \qquad [9]
\end{aligned}$$

Here functions C_i ($i = 1, \ldots, 32$) are given in Table 2. The equations for D's and V's are given in Table 3. Note that C's, V's, and D's are functions of the second pulse length t_2, whereas line intensities $\langle I_k^{m,n} \rangle$ are functions of the first pulse length t_1. In general, the density matrix of spin $\frac{7}{2}$ excited by an RF pulse is defined by 32 independent components denoted by $\langle I_k^{m,n} \rangle$). All of these are present in Eq. [9].

The profile of the central transition is defined as

$$F_x^{4,5}(t_1, t_2) + iF_y^{4,5}(t_1, t_2) = \langle 5|\rho_{\pi/2,\pi}(t_1, t_2)|4\rangle. \quad [10]$$

In the next section certain pulse sequences are considered which allow selective detection of some multiquantum transitions.

DETECTION OF MQ TRANSITIONS

The density matrix component $\langle 5|\rho_{\pi/2,\pi}(t_1, t_2)|4\rangle$ is complex (Eq. [9]), and thus the FID is detected by quadrature in both x and y channels (Eq. [10]). It should be noted that odd quantum coherences, developed during the first RF pulse, are detected in the x channel, whereas even quantum coherences and polarizations are detected in the y channel. Consider the following pulse sequence (sequence 1) (see Table 4). Applying a spin lock pulse sequence of this type (where the phases of the first and third pulses as well as the phase of the receiver after the second and fourth pulses are different by 180°) will result in the cancellation of the y component of the FID. However, the equation for the x component is simply deduced from Eq. [9] being twice as big as that given by Eqs. [9] and [10].

TABLE 2
The Functions $C_i(t_2)$ Used in Eqs. [13], [14], [15] for the Density Matrix Component ρ_{54} (t_1, τ, t_2)

$C_1 = Y_{1i}T_{1i}X_{2j}Z_{2j} \cos \omega_{ij}t_2$	$C_5 = Z_{1i}T_{1i}X_{2j}Y_{2j} \sin \omega_{ij}t_2$
$C_2 = Z_{1i}T_{1i}X_{2j}Y_{2j} \cos \omega_{ij}t_2$	$C_6 = Y_{1i}T_{1i}X_{2j}Z_{2j} \sin \omega_{ij}t_2$
$C_3 = T_{1i}T_{1i}X_{2j}X_{2j} \cos \omega_{ij}t_2$	$C_7 = X_{1i}T_{1i}X_{2j}T_{2j} \sin \omega_{ij}t_2$
$C_4 = X_{1i}T_{1i}X_{2j}T_{2j} \cos \omega_{ij}t_2$	$C_8 = T_{1i}T_{1i}X_{2j}X_{2j} \sin \omega_{ij}t_2$
$C_9 = Z_{1i}T_{1i}X_{2j}X_{2j} \cos \omega_{ij}t_2$	$C_{10} = Z_{1i}T_{1i}X_{2j}X_{2j} \sin \omega_{ij}t_2$
$C_{11} = T_{1i}T_{1i}X_{2j}Y_{2j} \cos \omega_{ij}t_2$	$C_{12} = T_{1i}T_{1i}X_{2j}Y_{2j} \sin \omega_{ij}t_2$
$C_{13} = Y_{1i}T_{1i}X_{2j}Y_{2j} \cos \omega_{ij}t_2$	$C_{14} = Y_{1i}T_{1i}X_{2j}Y_{2j} \sin \omega_{ij}t_2$
$C_{15} = Z_{1i}T_{1i}X_{2j}Z_{2j} \cos \omega_{ij}t_2$	$C_{16} = Z_{1i}T_{1i}X_{2j}Z_{2j} \sin \omega_{ij}t_2$
$C_{17} = Y_{1i}T_{1i}X_{2j}X_{2j} \cos \omega_{ij}t_2$	$C_{18} = Y_{1i}T_{1i}X_{2j}X_{2j} \sin \omega_{ij}t_2$
$C_{19} = T_{1i}T_{1i}X_{2j}Z_{2j} \cos \omega_{ij}t_2$	$C_{20} = T_{1i}T_{1i}X_{2j}Z_{2j} \sin \omega_{ij}t_2$
$C_{21} = X_{1i}T_{1i}X_{2j}Z_{2j} \cos \omega_{ij}t_2$	$C_{22} = X_{1i}T_{1i}X_{2j}Z_{2j} \sin \omega_{ij}t_2$
$C_{23} = Y_{1i}T_{1i}X_{2j}T_{2j} \cos \omega_{ij}t_2$	$C_{24} = Y_{1i}T_{1i}X_{2j}T_{2j} \sin \omega_{ij}t_2$
$C_{25} = X_{1i}T_{1i}X_{2j}Y_{2j} \cos \omega_{ij}t_2$	$C_{26} = X_{1i}T_{1i}X_{2j}Y_{2j} \sin \omega_{ij}t_2$
$C_{27} = Z_{1i}T_{1i}X_{2j}T_{2j} \cos \omega_{ij}t_2$	$C_{28} = Z_{1i}T_{1i}X_{2j}T_{2j} \sin \omega_{ij}t_2$
$C_{29} = X_{1i}T_{1i}X_{2j}X_{2j} \cos \omega_{ij}t_2$	$C_{30} = X_{1i}T_{1i}X_{2j}X_{2j} \sin \omega_{ij}t_2$
$C_{31} = T_{1i}T_{1i}X_{2j}T_{2j} \cos \omega_{ij}t_2$	$C_{32} = T_{1i}T_{1i}X_{2j}T_{2j} \sin \omega_{ij}t_2$

Note. The symbol $\Sigma_{i,j=1}^{4}$ in front of each term is omitted but assumed.

TABLE 3
The Functions $D_i(t_2)$ and $V_i(t_2)$ Used in Eq. [9]

$$D_1 = \frac{1}{2} X_{1i}X_{1j}T_{1i}T_{1j} \cos \psi_{ij}^{+}$$

$$D_2 = \frac{1}{2} T_{2i}T_{2j}X_{2i}X_{2j} \cos \psi_{ij}^{-}$$

$$D_3 = \frac{1}{2} Y_{1i}Y_{1j}T_{1i}T_{1j} \cos \psi_{ij}^{+}$$

$$D_4 = \frac{1}{2} Z_{2i}Z_{2j}X_{2i}X_{2j} \cos \psi_{ij}^{-}$$

$$D_5 = \frac{1}{2} Z_{1i}Z_{1j}T_{1i}T_{1j} \cos \psi_{ij}^{+}$$

$$D_6 = \frac{1}{2} Y_{2i}Y_{2j}X_{2i}X_{2j} \cos \psi_{ij}^{-}$$

$$D_7 = \frac{1}{2} T_{1i}T_{1j}T_{1i}T_{1j} \cos \psi_{ij}^{+}$$

$$D_8 = \frac{1}{2} X_{2i}X_{2j}X_{2i}X_{2j} \cos \psi_{ij}^{-}$$

$$V_1 = X_{1i}Y_{1j}T_{1i}T_{1j} \cos \psi_{ij}^{+}$$

$$V_2 = Z_{2i}T_{2j}X_{2i}X_{2j} \cos \psi_{ij}^{-}$$

$$V_3 = T_{2i}X_{2j}X_{2i}X_{2j} \cos \psi_{ij}^{-}$$

$$V_4 = X_{1i}T_{1j}T_{1i}T_{1j} \cos \psi_{ij}^{+}$$

$$V_5 = Z_{1i}X_{1j}T_{1i}T_{1j} \cos \psi_{ij}^{+}$$

$$V_6 = T_{2i}Y_{2j}X_{2i}X_{2j} \cos \psi_{ij}^{-}$$

$$V_7 = Z_{1i}Y_{1j}T_{1i}T_{1j} \cos \psi_{ij}^{+}$$

$$V_8 = Y_{2i}Z_{2j}X_{2i}X_{2j} \cos \psi_{ij}^{-}$$

$$V_9 = Y_{1i}T_{1j}T_{1i}T_{1j} \cos \psi_{ij}^{+}$$

$$V_{10} = Z_{2i}X_{2j}X_{2i}X_{2j} \cos \psi_{ij}^{-}$$

$$V_{11} = T_{1i}Z_{1j}T_{1i}T_{1j} \cos \psi_{ij}^{+}$$

$$V_{12} = Y_{2i}X_{2j}X_{2i}X_{2j} \cos \psi_{ij}^{-}$$

$$V_{13} = X_{1i}Y_{1j}T_{1i}T_{1j} \sin \psi_{ij}^{+}$$

$$V_{14} = T_{2i}Z_{2j}X_{2i}X_{2j} \sin \psi_{ij}^{-}$$

$$V_{15} = T_{1i}X_{1j}T_{1i}T_{1j} \sin \psi_{ij}^{+}$$

$$V_{16} = T_{2i}X_{2j}X_{2i}X_{2j} \sin \psi_{ij}^{-}$$

$$V_{17} = Z_{1i}X_{1j}T_{1i}T_{1j} \sin \psi_{ij}^{+}$$

$$V_{18} = Y_{2i}T_{2j}X_{2i}X_{2j} \sin \psi_{ij}^{-}$$

$$V_{19} = Y_{1i}Z_{1j}T_{1i}T_{1j} \sin \psi_{ij}^{+}$$

$$V_{20} = Y_{2i}Z_{2j}X_{2i}X_{2j} \sin \psi_{ij}^{-}$$

$$V_{21} = Y_{1i}T_{1j}T_{1i}T_{1j} \sin \psi_{ij}^{+}$$

$$V_{22} = X_{2i}X_{2j}X_{2i}X_{2j} \sin \psi_{ij}^{-}$$

$$V_{23} = Z_{1i}T_{1j}T_{1i}T_{1j} \sin \psi_{ij}^{+}$$

$$V_{24} = X_{2i}Y_{2j}X_{2i}X_{2j} \sin \psi_{ij}^{-}$$

Note. The symbol $\Sigma_{i,j=1}^{4}$ in front of each term is omitted but assumed. $\psi_{ij}^{+} = (\omega_{1i} - \omega_{1j})t_2$, $\psi_{ij}^{-} = (\omega_{2i} - \omega_{2j})t_2$.

Thus the density matrix component of the central transition for sequence 1 is

$$\langle 5|\rho^{seq1}(t_1, t_2)|4\rangle = 2\,\mathrm{Re}\{\langle 5|\rho_{\pi/2,\pi}(t_1, t_2)|4\rangle\}. \quad [11]$$

Sequence 1 can be modified such that the phase of the receiver after second and fourth pulses remain unchanged. This new sequence (sequence 2 from Table 4) results in the cancellation of the x component of the FID. At the same time the y component is twice as big as that produced by the sequence which consists of the pulses 1 and 2 only. The equation for the density matrix component of the central transition becomes

$$\langle 5|\rho^{seq1}(t_1, t_2)|4\rangle = 2i\,\mathrm{Im}\{\langle 5|\rho_{\pi/2,\pi}(t_1, t_2)|4\rangle\}. \quad [12]$$

From our previous results (*12*), the density matrix component of the central transition for the sequence (sequence 3 from Table 4) is designed for so called even quantum detection (rotary echo type) and is given by

$$\begin{aligned}\langle 5|\rho^{Seq.3}(t_1, t_2)|4\rangle = 2i\{&\langle I_z^{3,6}\rangle C_5 + \langle I_z^{2,7}\rangle C_6 \\ &+ \langle I_z^{1,8}\rangle C_7 + \langle I_z^{4,5}\rangle C_8 + \langle I_x^{3,5}\rangle (C_{10} - C_{12}) \\ &+ \langle I_x^{2,6}\rangle (C_{14} - C_{16}) + \langle I_x^{2,4}\rangle (C_{18} + C_{20}) \\ &+ \langle I_x^{1,7}\rangle (C_{22} - C_{24}) + \langle I_x^{1,3}\rangle (C_{26} + C_{28}) \\ &+ \langle I_x^{1,5}\rangle (C_{30} - C_{32}) + \langle I_y^{3,5}\rangle (C_9 + C_{11}) \\ &+ \langle I_y^{2,6}\rangle (C_{13} + C_{15}) + \langle I_y^{2,4}\rangle (C_{17} - C_{19}) \\ &+ \langle I_y^{1,7}\rangle (C_{21} + C_{23}) + \langle I_y^{1,3}\rangle (C_{25} - C_{27}) \\ &+ \langle I_y^{1,5}\rangle (C_{29} + C_{31})\}. \end{aligned} \quad [13]$$

TABLE 4
Pulse Sequences Used in This Paper

Sequence	Q_1	Q_2	Q_R
1	y	$-x$	y
	$-y$	$-x$	$-y$
2	y	$-x$	y
	$-y$	$-x$	y
3	$-x$	$-x$	y
	x	$-x$	y
4	y	$-x$	y
	$-y$	$-x$	y
	$-x$	$-x$	y
	x	$-x$	y
5	y	$-x$	$-y$
	$-y$	$-x$	$-y$
	$-x$	$-x$	y
	x	$-x$	y

Note. Q_1, Q_2, and Q_R indicate the phase of the first and second pulse and the receiver.

Sequences 2 and 3 can be combined into sequence 4 (Table 4), such that the resultant magnetization vector is aligned with the z axis, and the equation for the density matrix component of the central transition for the sequence 4 is

$$\begin{aligned}\langle 5|\rho^{Seq.4}(t_1, t_2)|4\rangle = 4i\{&\langle I_z^{3,6}\rangle C_5 + \langle I_z^{2,7}\rangle C_6 \\ &+ \langle I_z^{1,8}\rangle C_7 + \langle I_z^{4,5}\rangle C_8 + \langle I_x^{2,6}\rangle (C_{14} - C_{16}) \\ &+ \langle I_x^{1,5}\rangle (C_{30} - C_{32}) + \langle I_y^{2,6}\rangle (C_{13} + C_{15}) \\ &+ \langle I_y^{1,5}\rangle (C_{29} + C_{31})\}. \end{aligned} \quad [14]$$

Thus 4-quantum coherences, developed during the first pulse, are detected. However, if sequences 2 and 3 are combined into sequence 5 (Table 4) such that the phase of the receiver in Sequence 2 is changed by 180°, then double quantum coherences developed during the first pulse are detected,

$$\begin{aligned}\langle 5|\rho^{Seq.5}(t_1, t_2)|4\rangle = 4i\{&\langle I_x^{3,5}\rangle (C_{10} - C_{12}) \\ &+ \langle I_x^{2,4}\rangle (C_{18} + C_{20}) + \langle I_x^{1,3}\rangle (C_{26} + C_{28}) \\ &+ \langle I_y^{3,5}\rangle (C_9 + C_{11}) + \langle I_y^{2,4}\rangle (C_{17} - C_{19}) \\ &+ \langle I_y^{1,3}\rangle (C_{25} - C_{27})\}. \end{aligned} \quad [15]$$

It should be noted here that the response of the system in question becomes less complicated as the number of pulses increases. However, at the same time the signal-to-noise ratio decreases which can limit the applicability of long pulse sequences for powders. On the other hand these pulse sequences allow the determination of quadrupolar coupling in a single crystal, and the quadrupolar coupling constant and asymmetry parameter in powders. These values, obtained using the variety of pulse sequences, should be consistent and this improves the level of confidence of our results. The important feature of sequence 5 is that it drastically reduces spurious signals (*18*) generated by the NMR probe for nuclei with small gyromagnetic ratios. When used in NMR with no quadrupolar splitting, this sequence places the magnetization vector along the z axis and causes no response. However for quadrupolar nuclei, the signal is detected due to multiquantum coherences developed during the first pulse.

Figures 1–4 show the theoretical line intensities for sequences 1, 2, 4, and 5 calculated for different ratios of ω_Q/ω_1.

A ''Maple'' program which numerically computes the

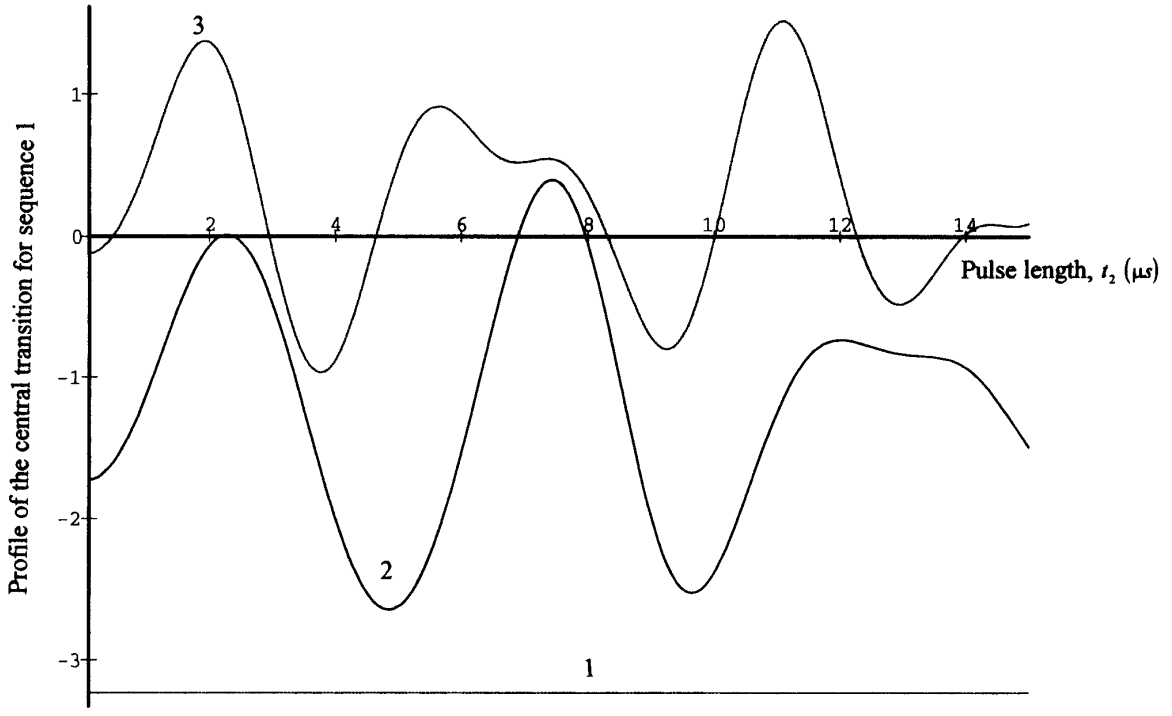

FIG. 1. The response to sequence 1 as the function of the second pulse length, t_2 for $t_1 = 3\ \mu s$, $\omega_1/2\pi = 50$ kHz and (1) $\omega_Q/2\pi = 0$ kHz, (2) $\omega_Q/2\pi = 50$ kHz, (3) $\omega_Q/2\pi = 100$ kHz.

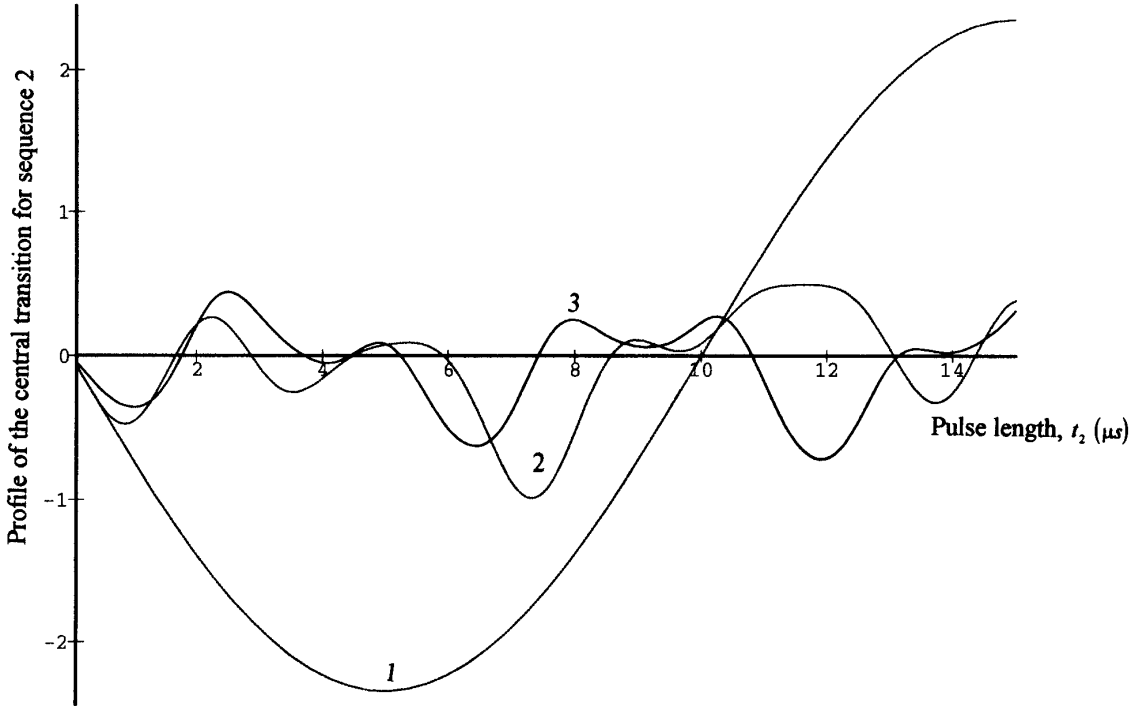

FIG. 2. The response to sequence 2 as the function of the second pulse length, t_2 for $t_1 = 3\ \mu s$, $\omega_1/2\pi = 50$ kHz and (1) $\omega_Q/2\pi = 0$ kHz, (2) $\omega_Q/2\pi = 50$ kHz, (3) $\omega_Q/2\pi = 100$ kHz.

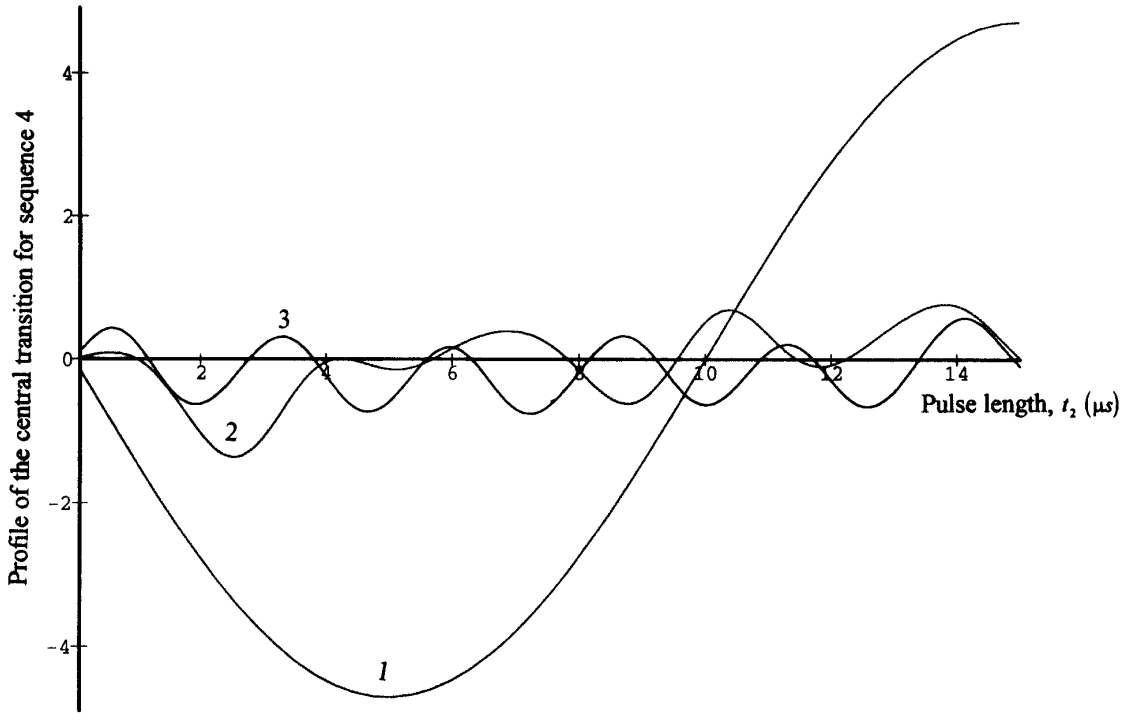

FIG. 3. The response to sequence 4 as the function of the second pulse length, t_2 for $t_1 = 3\ \mu s$, $\omega_1/2\pi = 50$ kHz and (1) $\omega_Q/2\pi = 0$ kHz, (2) $\omega_Q/2\pi = 50$ kHz, (3) $\omega_Q/2\pi = 100$ kHz.

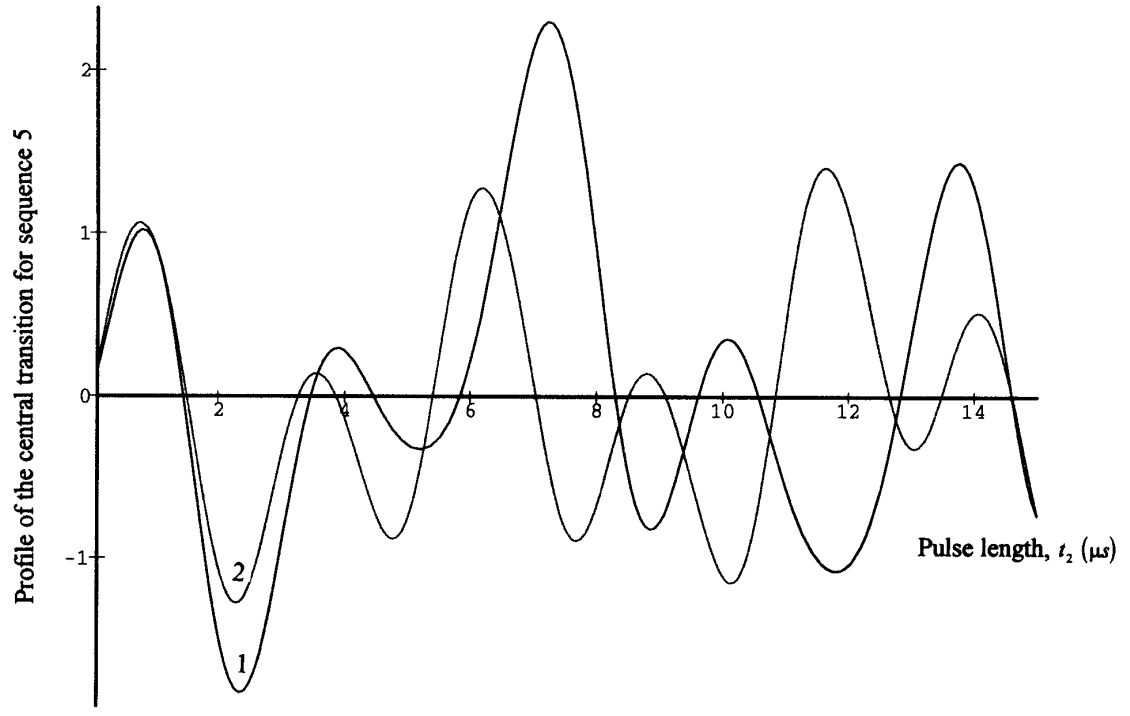

FIG. 4. Same as described in the legend to Fig. 1 for Sequence 5 but (1) $\omega_Q/2\pi = 50$ kHz, (2) $\omega_Q/2\pi = 100$ kHz.

responses to sequences 1 and 2 for half integer spins of arbitrary amplitude is supplied in Appendix.

CONCLUSIONS

The response of a spin $\frac{7}{2}$ to spin lock excitation and to a variety of two-pulse sequences involving the combination of rotary echo and spin lock sequences is presented. The first-order quadrupole is retained throughout the calculation. Our primary focus is on the central transition as it represents the main signal of detection in powders. Also calculated is the density matrix of any half-integer spin after an RF pulse of arbitrary phase. This shows that when the phase of the pulse is shifted by ϕ, the phases of m-quantum coherences change by $m\phi$. However, these are not detected except for the case of $m = 1$. Use of two-pulse experiments allows the detection of multiquantum coherences through SQ coherences after the second pulse. It is proven here that DQ coherences can be selectively detected using appropriate phase cycling. In this case, the central line intensity is a function of both pulse lengths, the quadrupolar coupling and the amplitude of the RF pulse. Fitting curves representing the central line intensities as the function of the duration of one of the pulses allows the determination of quadrupolar parameters. Finally, we remark that our analytical solution for the eigenvalue–eigenfunction problem (*17*) can be used in the analysis of (*19*) for spin $\frac{7}{2}$.

APPENDIX

```
# this program calculates the two-pulse response for spin i
#solid state nmr

# set spin magnitude to 7/2
i:=7/2;
nsize:=2*i+1;
i_plus:=array(sparse,1..nsize,1..nsize):
i_minus:=array(1..nsize,1..nsize):
i_x:=array(1..nsize,1..nsize):
i_y:=array(1..nsize,1..nsize):
i_z:=array(sparse,1..nsize,1..nsize):
i_q:=array(sparse,1..nsize,1..nsize):

  i_row:=1;
  for m from -i to i-1 do
  i_plus[i_row,i_row+1]:=evalf(sqrt((i+m+1)*(i-m)));
  i_q[i_row,i_row]:=i*(i+1)-3*m**2;
  i_z[i_row,i_row]:=-m;
  i_row:= i_row + 1;
  od;
  i_z[i_row,i_row]:= -i;
  i_q[i_row,i_row]:=i*(i+1)-3*i**2;

i_minus:=evalm(transpose(i_plus));
i_x:=evalm(i_plus + i_minus)/2;
i_y:=evalm((i_plus - i_minus)/(2*I));

with(linalg);

# set quadrupolar coupling to 50 kHz and rf amplitude to
  50 kHz

wq:=evalf(0.050*2*Pi);
wl:=evalf(0.050*2*Pi);

# set duration of the first pulse to 3 microsec and phase to
  pi/2
t1:=3.0;
phi:=Pi/2;

hq:=evalm(-wq/3*i_q-wl*i_x);
hql:=evalm(-wq/3*i_q+wl*i_x);
hqq:=evalm(i_z);

u1:=exponential(hq,-I*t1);
u_1:=exponential(hq,I*t1);
u2:=exponential(hqq,-I*phi);
u_2:=exponential(hqq,I*phi);

ro1:=evalm(u2&*u1&*i_z&*u_1&*u_2);

u3:=exponential(hq1,-I*t);
u_3:=exponential(hq1,I*t);

sum:=0;
n1:=nsize/2+1;
n2:=nsize/2;

for i from 1 to nsize do
for j from 1 to nsize do

  term:=u3[n1,i]*ro1[i,j]*u_3[j,n2];
  sum:=sum+term;

od;
od;

answer1:=Im(sum);
answer2:=Re(sum);
# time t scale is in microseconds
plot(answer1,t=0.01..15);
plot(answer2,t=0.01..15);
```

ACKNOWLEDGMENT

S.Z.A. acknowledges useful discussions with Dr. Lixin Tao.

REFERENCES

1. G. Bodenhausen, *Prog. NMR Spectrosc.* **14,** 137 (1981).
2. S. Vega, T. W. Shattuck, and A. Pines, *Phys. Rev. A* **22,** 1980.
3. S. Vega, T. W. Shattuck, and A. Pines, *Phys. Rev. Lett.* **37,** 43 (1976).
4. A. Wokaun and R. R. Ernst, *J. Chem. Phys.* **67,** 1752 (1977).

5. M. E. Stoll, E. K. Wolf, and M. Mehring, *Phys. Rev. A* **17,** 1561 (1978).
6. H. Hatanaka and T. Hashi, *Phys. Rev. B* **27,** 4095 (1983).
7. H. Hatanaka and Takahama, *Phys. Rev. B* **47,** 3213 (1993).
8. W. D. Rooney, T. M. Barbara, and C. S. Springer, Jr., *J. Am. Chem. Soc.,* **110,** 674 (1988).
9. P. P. Man, *Mol. Phys.* **76,** 1119 (1992).
10. D. C. Newitt and E. L. Hahn, *J. Magn. Reson. A* **106,** 140 (1994).
11. P. P. Man, *Sol. State NMR* **2,** 165 (1993).
12. S. Z. Ageev, P. P. Man, Fraissard, and B. C. Sanctuary, *Mol. Phys.* (1996), in press.
13. P. P. Man, *Z. Naturforsch. A* **49,** 89 (1994).
14. S. Z. Ageev, P. P. Man, and B. C. Sanctuary, *Mol. Phys.* **88,** 1277 (1996).
15. P. P. Man, *J. Magn. Reson. A* **113,** 40 (1995).
16. L. Frydman, J. S. Harwood, *J. Am. Chem. Soc.* **117,** 5367 (1995).
17. S. Z. Ageev and B. C. Sanctuary, *Mol. Phys.* **84,** 835 (1995).
18. I. P. Gerothanassis, *Prog. NMR Spectrosc.,* **19,** 1987 (1987).
19. S. Ding and C. A. McDowell, *J. Magn. Reson. A* **112,** 36 (1995).